Thermally Stable Redox Noninnocent Bathocuproine-Iron Complex for Cycloaddition Reactions

Mae Féo, Nikki Bakas, Aleksa Radović, William Parisot, Anne Clisson, Lise-Marie Chamoreau, Mansour Haddad, Virginie Ratovelomanana-Vidal, Michael L Neidig, Guillaume Lefèvre

A Thermally-Stable Redox Non-Innocent Bathocuproine-Iron Complex for Cycloaddition Reactions

Mae Féo,[+[a]] *Nikki Bakas,*[+[b]] *Aleksa Radović,*[[b]] *William Parisot,*[[a]] *Anne Clisson,*[[a]] *Lise-Marie Chamoreau,*[[c]] *Mansour Haddad,*[[a]] *Virginie Ratovelomanana-Vidal,*[[a]] *Michael L. Neidig**[[b,d]] *and Guillaume Lefèvre**[[a]]

[a] Chimie ParisTech, PSL University, CNRS, Institute of Chemistry for Life and Health Sciences, CSB2D, 75005 Paris, France

[b] Department of Chemistry, University of Rochester, Rochester, NY, 14627, USA

[c] Sorbonne Université, CNRS, Institut Parisien de Chimie Moléculaire, F-75252, Paris, France

[d] Inorganic Chemistry Laboratory, Department of Chemistry, University of Oxford, South Parks Road, Oxford OX1 3QR, United Kingdom

[+] These authors contributed equally to this work.

ABSTRACT. In this work, we aim to design formally iron(0) complexes combined with a phenanthroline-type ligand (phen) and investigate their utility in cycloaddition catalysis. Owing to the strong non-innocence of the phen scaffold, its ligation to reduced iron oxidation states classically affords particularly unstable species. The reported examples of such well-defined coordination complexes are thus particularly scarce. We demonstrate herein that a strategic steric

protection of the C4 and C7 positions of the phen ring leads to neutral $(N,N)_2Fe$ species which exhibits an unprecedented thermal and kinetic stability, amenable to its easy use as an *in situ* generated precursor in catalytic processes. The electronic structure of this non-innocent complex has been fully rationalized, and its promising catalytic activity in alkyne [2+2+2] cyclizations is discussed. Given its intrinsic thermal stability due to the non-innocent behavior of the (N,N) ligand, $(N,N)_2Fe$ appears to be an efficient dormant state of the catalytic process, precluding desactivation of iron as non-reactive aggregates.

KEYWORDS. Iron, non-innocence, phenanthrolines, cycloaddition, mechanisms.

INTRODUCTION. Base metal complexes containing redox non-innocent ligands continue to attract widespread interest for applications in catalysis. Of particular interest are iron complexes with redox non-innocent ligands, which have been widely explored for the development of more sustainable catalytic methods. Building upon the early work of Brookhart and Gibson utilizing bis(imino)pyridine- or pyridinediimine (PDI)-iron complexes for the catalysis of olefin polymerization (Scheme 1a)[1] and Wieghardt and Budzelaar establishing the "redox active" nature of PDI ligands,[2] Chirik demonstrated the utility of the PDI-iron complex as a catalyst for hydrogenation and hydrosilylation of olefins[3] and the cyclization of enynes and dienes (Scheme 1b).[4] Other examples of this catalyst's versatility include butadiene dimerization by Ritter,[5] regio- and enantioselective cycloaddition of dienes by Cramer,[6] and hydroboration of carbonyl compounds by Wolf.[7]

Central to the catalytic utility of such iron complexes is the potential for the pre-catalysts and intermediates to undergo redox processes that involve changes in the redox state of the ligand, as well as the metal.[8] The properties of these redox non-innocent ligands are attributed to their lower-lying LUMOs, with respect to redox innocent ligands, increasing the possibility for the electrons to be in ligand orbitals. Not only does this make the electronic structure challenging to discern, but it also contributes to their unique reactivities. For example, when the formal reduction of the PDI-iron complex occurs, it is the PDI ligand that is reduced rather than the iron, thus resulting in $(PDI)Fe^{II}$ transforming to $(PDI^{2-})Fe^{II}$ instead of $(PDI)Fe^{0}$. The non-innocent ligands thus act as formal electron reservoirs, which can contribute to the generation of reduced platforms displaying a better stability than complexes involving low metal oxidation states with no metal-to-ligand charge delocalization. Such ligands are therefore particularly appealing for catalytic applications requiring the formation of formally reduced metal complexes.

While PDI and diimmine ligands have been widely explored in the literature as potential redox non-innocent ligands in catalysis with iron (*vide supra*), simpler neutral (N,N) ligands such as phenanthroline (phen) and substituted phen have yet to be studied to the same extent.[9] Such ligands have been studied in detail for nickel chemistry, where they have been demonstrated to be very effective intermediates in various nickel-catalyzed cross-coupling reactions by Diao and co-workers (Scheme 1c).[9c] In contrast to nickel, studies of phen-type ligands with iron have focused predominately on complexes with a (+II) oxidation, and the coordination chemistry as well as the catalytic applications of low iron oxidation states associated with those ligands still have to be explored. Amongst the scarce examples of processes involving iron catalysts stabilized by phen-type ligands in a reducing medium, Zhu and Hu described a highly efficient

alkene hydrosilylation system, relying on the association of an iron(II) salt with 2,9-diarylphenanthroline ligands. $PhSiH_3$ is used as a Si-H bond source, and EtMgBr as an external reductant (Scheme 1d).[9d] The performances of a series of non-innocent N-based ligands (PDI, bipyridines, phenanthrolines, phosphine-bipyridines) applied to alkene hydrogenation were also assessed by Zhu.[9e] In this context, one must keep in mind that a high degree of non-innocence can strongly destabilize such reduced complexes, since it will impart the latter a reactivity in-between that of a neutral species and that of a radical anion.

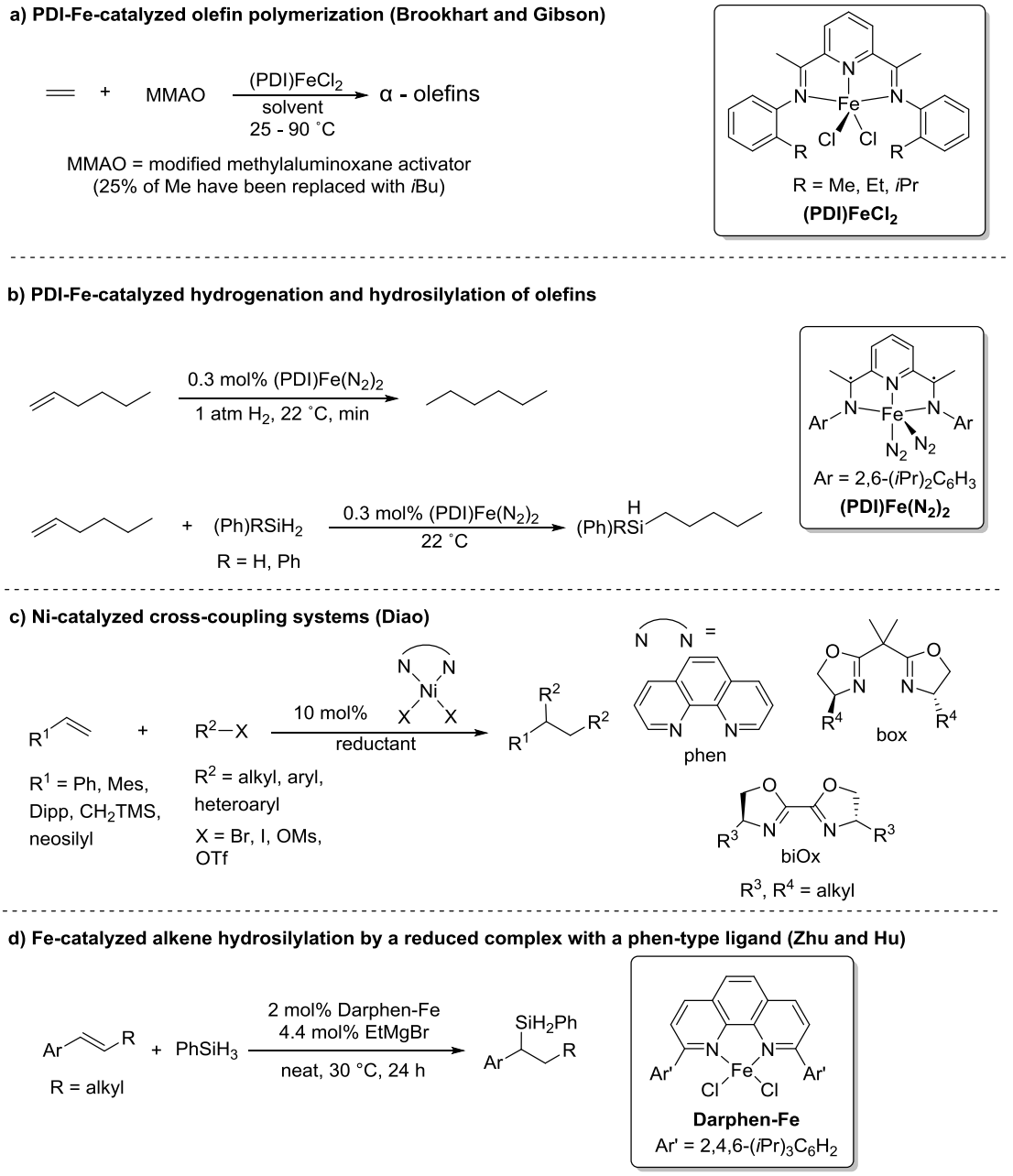

Scheme 1: a) PDI-Fe catalysts developed by Brookhart and Gibson; b) Non-innocent PDI system (Ar = 2,6-(iPr)$_2$C$_6$H$_3$) developed by Chirik; c) example of Ni-catalyzed coupling reactions developed by Diao; d) alkene hydrosilylation mediated by a phen-type-ligand stabilized iron salt in a reducing medium by Zhu and Hu.

The case of the phen ligand is particularly representative. Energetically easily accessible, the two lowest unoccupied levels (LUMO and LUMO+1) of phen display an important contribution on the C4 and C7 positions (Scheme 2a). Therefore, in a complex associating a ligand derived from phen with a strongly reducing metal, those positions acquire a significant radical character, and can thus evolve towards usual one-electron reactivity pathways.[10] A great care must thus be taken regarding the control of the metal-to-ligand charge transfer induced by this non-innocent behavior, since it can have a dramatic impact on the stability of the complex. Recently, Anderson and co-workers explored systematically 2,9-dimethyl-1,10-phenanthroline, more commonly referred to as neocuproine (L' herein), as a potentially redox non-innocent ligand to iron and cobalt.[11] Thorough characterization of the 2:1 neocuproine:metal neutral L'_2M (M = Co, Fe) complexes revealed them to be Fe^{2+} and Co^{2+} with two ligand-based radicals. To date, however, this hasn't been expanded upon with other ligand types nor has the potential reactivity of these complexes been explored for catalysis.

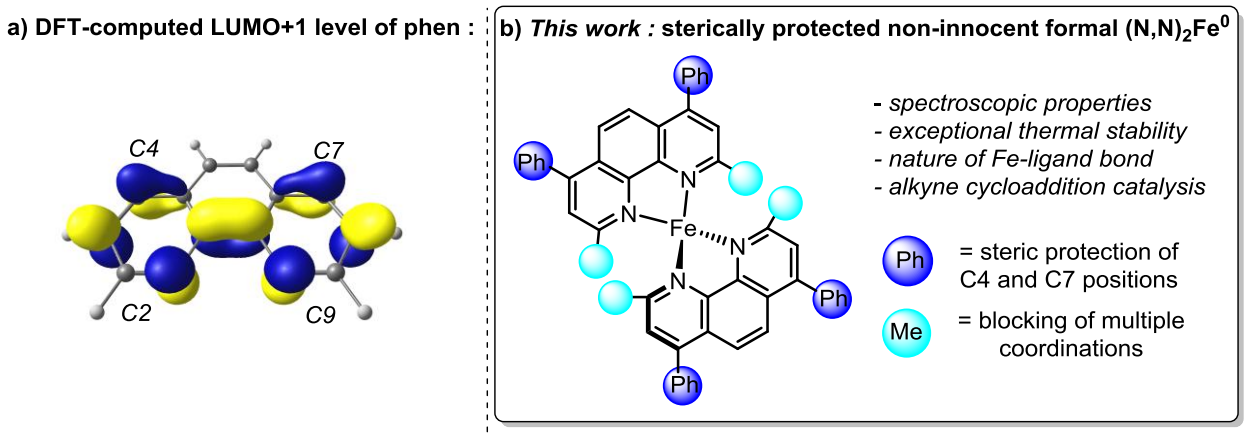

Scheme 2: a) DFT-computed LUMO+1 level of phen; b) neutral $(bathocuproine)_2Fe$ (L_2Fe) complex investigated in this work.

Inspired by this prior work, we aimed to more broadly explore such phen-based ligands with iron in formally low oxidation states with a particular goal of exploiting such complexes in catalytic transformations for formation of new C-C bonds. By adding phenyl groups at the C4 and C7 positions of the neocuproine ligand, it was hypothesized that the addition of the steric hinderance might prevent the occurrence of chemical transformation on those sites (Scheme 2b). Herein we synthesize and characterize the ligation of 2,9-dimethyl-4,7-diphenyl-1,10-phenanthroline (bathocuproine = L) to iron in the form of L_2Fe, resulting in a new homoleptic formal Fe^0 complex, actually described as an iron(II) with two ligand-based radicals. L_2Fe complex displays an unprecedented thermal stability in solution, as the substitution of the C4 and C7 positions prevents decomposition pathways induced by the ligand non-innocence. This species is a unique example of thermally stable neutral complex involving ligation of an iron center by a phen-type ligand. Highlighting its possible use for catalytic applications, this new iron complex is demonstrated to be an atom-efficient catalyst in [2+2+2] alkyne cyclotrimerizations and cross-cycloisomerizations of 1,6-diynes with alkyne partners.

RESULTS AND DISCUSSION.

Synthesis and Characterization of Well-Defined Bathocuproine-Iron Complexes

Initial studies focused on the synthesis and characterization of bathocuproine-ligated iron complexes. A common practical starting material we set out to make was coordination of the ligand, in this case bathocuproine, to an iron(II) precursor. The reaction of equal mol amounts of $FeCl_2$ and bathocuproine in THF at 80 °C during 16 h, followed by recrystallization at room

temperature, resulted in dark orange needles (97% yield). The crystals were analyzed by X-ray diffraction (XRD) and identified to be (bathocuproine)$Fe^{II}Cl_2$ ($LFeCl_2$, **1**), a distorted tetrahedral bis-halide complex (Figure 1). Solid-state 80 K ^{57}Fe Mössbauer spectroscopy of **1** displays an isomer shift (δ) = 0.89 mm/s and electric quadrupole splitting ($|\Delta E_Q|$) = 2.60 mm/s (Figure S1a) consistent with a high-spin iron(II) species, which was further confirmed by SQUID magnetometry experiments (Figure S1b). In line with this, the ^1H NMR spectrum of **1** displays paramagnetic resonances in the 10-60 ppm and -25 ppm areas (Figure S1c). Utilizing **1** as starting material, we sought after accessing reduced iron species with bathocuproine as the ligand.

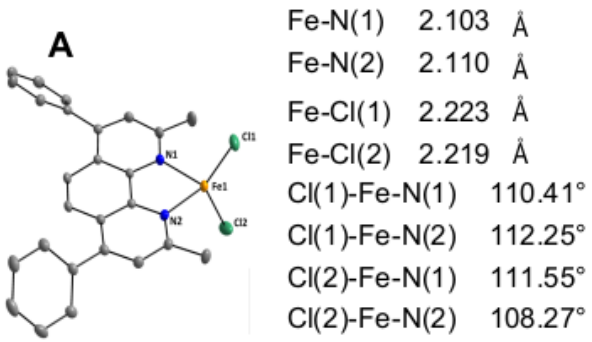

Figure 1: Crystal structure of $LFeCl_2$ (**1**) (hydrogen atoms omitted for clarity, ellipsoids drawn at 30% probability level).

To form a reduced iron species, an alkenyl Grignard reagent was chosen as the reductant because it was hypothesized that the 1,3-diene formed by the reduction of **1** could act as an η^4-ligand to the reduced iron. The reaction of 2 equiv. of 2-methyl-1-propenylmagnesium bromide (Me_2C=CHMgBr, noted as RMgBr) with **1** yielded the formation of 1,3-diene $Me_2CCHCHCMe_2$ detected by GC-MS, confirming the two-electron reduction by reductive elimination of a transient bishydrocarbyl $LFe^{II}(R)_2$ intermediate. The reduced species was analyzed by Mössbauer spectroscopy. Upon the addition of the alkenyl Grignard, the pale orange solution of

^{57}Fe-labeled **1** in THF immediately turned dark purple and displayed a major iron species (50% of total iron, Figure S4) with parameters of δ = 0.77 mm/s and electric quadrupole splitting $|\Delta E_Q|$ = 1.21 mm/s. Crystals of the major iron species suitable for XRD were obtained; the resulting dark purple cubes were identified to be a distorted tetrahedral bis(bathocuproine) iron complex, L_2Fe (**2**) (Figure 2A). SQUID magnetometry of **2** displays paramagnetic behavior with a μ_{eff} = 2.8(4) B.M. at 298 K and no spin transitions observed at low temperatures (Figure S2a). In line with this, the ^{1}H NMR of complex **2** exhibits paramagnetic resonances in the 25-120 ppm and -70 ppm areas (Figure S2b). Note that the synthesis of **2** can be quantitatively performed by reduction of **1** with 2 equiv. RMgBr in the presence of a second equiv. of bathocuproine L at 20 °C during 20 min (Figure 2B, see Figures S3-S5 for ^{1}H NMR and Mössbauer reduction monitoring). Mössbauer monitoring moreover suggests the possible formation of a transient iron(II)-alkenyl intermediate involved in the formation of **2** (Figure S5a), based on comparison with already reported similar compounds.[12]

It should also be noted that complex **2** can be formed with KC_8 as the reductant (2 equiv. of KC_8 used per mole of **1**). Solid-state Mössbauer spectroscopy of crystalline **2** generated parameters δ = 0.75 mm/s and electric quadrupole splitting $|\Delta E_Q|$ = 1.19 mm/s (Figure 2C), confirming the major *in situ* generated iron species discussed earlier.

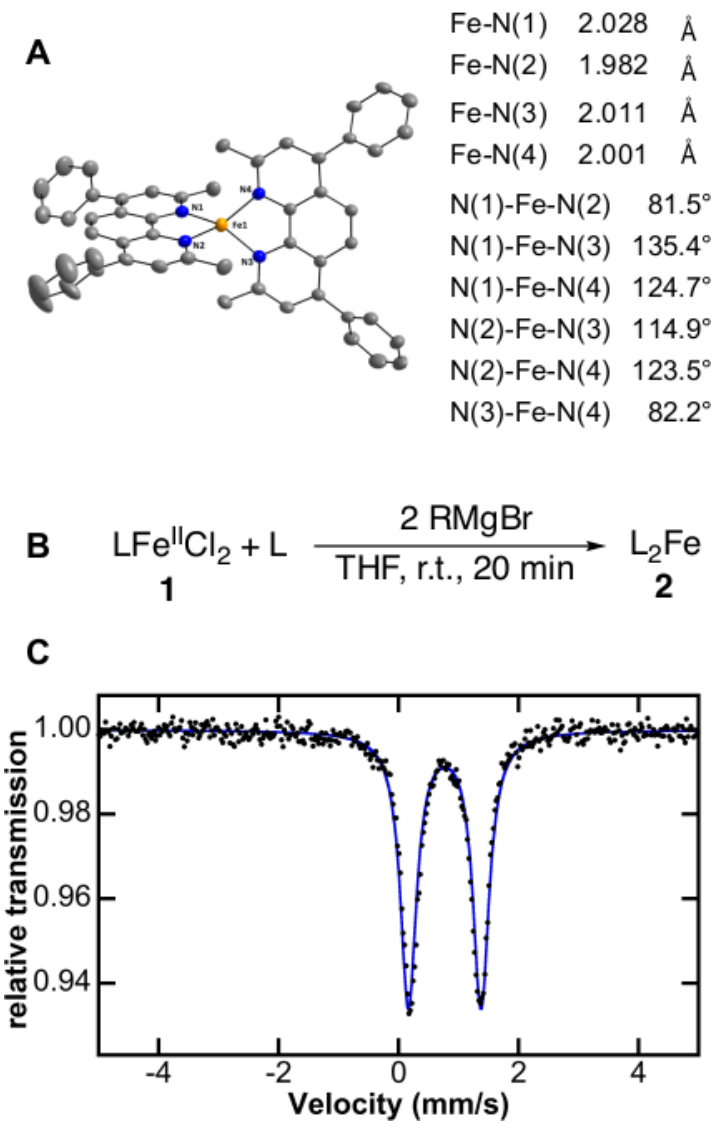

Figure 2: A) Crystal structure of L_2Fe (**2**) (hydrogen atoms omitted for clarity, ellipsoids drawn at 30% probability level); B) synthesis of **2** by reduction of **1**; and C) 80 K ^{57}Fe Mössbauer spectrum of solid **2** with $\delta = 0.75$ mm/s and $|\Delta E_Q| = 1.19$ mm/s.

Comparison of the metric parameters in **1** ($LFeCl_2$) and **2** (L_2Fe) (Figure 1 and Figure 2A) reveals that the average Fe─N distance shortens upon the reduction process (Fe─N1 = 2.103 Å, Fe─N2 = 2.110 Å in **1**; Fe─N1 = 2.028 Å, Fe─N2 = 1.982 Å, Fe─N3 = 2.011 Å, Fe─N4 = 2.001 Å in **2**), and that the (N-Fe-N) bite angles increase from **1** to **2** (N1-Fe-N2 = 78.18° in **1**; N1-Fe-

N2 = 81.51°, N3-Fe-N4 = 82.18° in **2**). Even if the nature of the coordination sphere strongly changes after the two-electron reduction of **1**, those data indicate that the metal center is closer to the ligand in **2** than in **1**, suggesting that a stronger metal-ligand interaction developed in the reduced complex **2**.

Before using **2** in a catalytic reaction, it was first important to determine its stability. Two strategies can be envisioned for using such a reduced complex in a catalytic reaction: either it can be generated *in situ*, by reduction of a suitable precursor (Grignard reagents being commonly used in synthetic chemistry to do so), or it can be synthesized and purified prior to its use. In the latter case, standard glovebox conditions are usually mandatory, which can preclude a routine use of such species in organic synthetic chemistry. Therefore, the compared stabilities of reduced complex **2** and of its neocuproine analogue **2'** utilized by Anderson[11] were investigated after *in situ* generation using a Grignard reagent on one hand, and after synthesis and purification on the other hand.

In situ generated THF solution of **2** (sealed in a J-Young tube) was proven to be stable up to 430 K, with thermal degradation only being observed starting at 370 K (Figure 3a, purple dots). The stability of pure, isolated **2** in THF is significantly higher, as 60% of **2** is still detected by ^{1}H NMR after heating at 510 K (Figure S10). We believe the stability of complex **2** can be attributed to the strong interactions developing between the bathocuproine reduced ligand with the iron(II) ion, as well as to the steric protection brought by the C4 and C7 phenyl groups. This thus prevents any ligand-based decomposition pathway induced by the non-innocence of the bathocuproine ligand. When comparing these results to the neocuproine analogue (L'$_2$Fe or **2'**), *in situ* generated complex **2** remains stable at higher temperatures, while less than 10% of **2'**

remains after heating at 350 K (Figure 3a, red dots). Thermal stability of isolated complex **2'** is also enhanced compared to that of *in situ* generated **2'**, but decomposition is also observed at lower temperatures than for isolated **2**, attesting to a less marked stability of **2'** (20% of **2'** *vs* 70% of **2** remaining in solution at 450 K, Fig. S10). Since **2'** has no steric bulk at the C4 and C7 positions, this further supports our hypothesis that the phenyl groups are ensuring the stability of **2**. Similar trends are observed when kinetic stabilities of **2** and **2'** *in situ* generated by reduction of the (L/L')$Fe^{II}Cl_2$ precursors (**1** or **1'**) with a Grignard in the presence of a second equivalent of L or L' are monitored at room temperature (Figure 3b): whereas **2** proved to be stable for more than 2 weeks in solution at 290 K, less than 35% of **2'** was recovered after 3 days at this temperature. **2** is thus an unique example of non-innocent iron complex with an extremely stabilizing platform, allowing an efficient storage of two electrons after reduction performed at the ferrous stage, and whose remarkable stability after *in situ* generation can pave the way to further applications in routine synthetic chemistry.

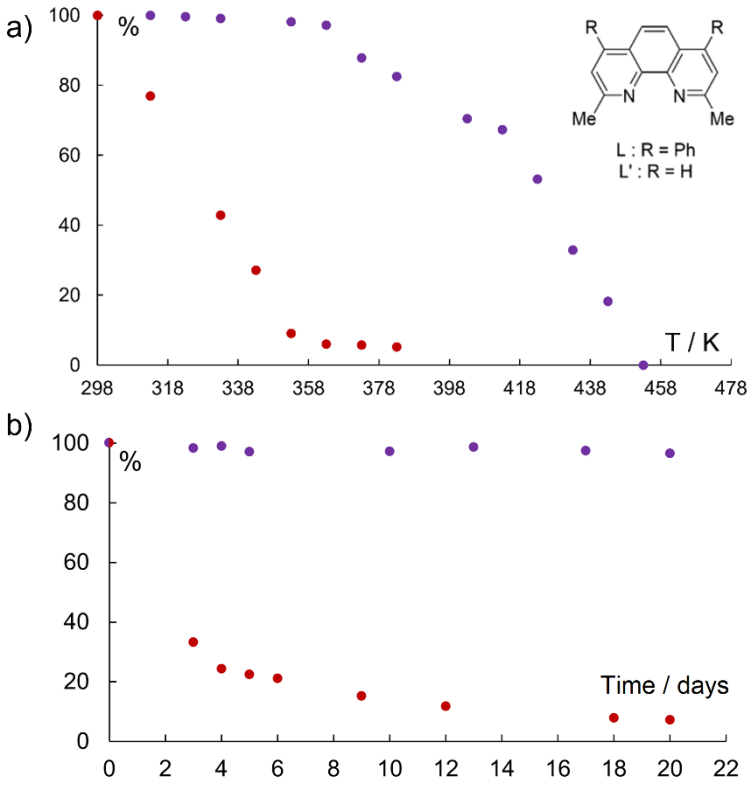

Figure 3: a) thermal and b) kinetic stability (at 290 K) of complexes **2** (L_2Fe, purple dots) and **2'** (L'_2Fe, dark red dots) *in situ* generated in THF d_8 (sealed J. Young tube) by reduction of (L/L')$FeCl_2$ (2 equiv. Me_2C=CHMgBr) in the presence of one equivalent of L (**2**) or L' (**2'**); relative ratios determined by ^{1}H NMR.

Mirroring the experimental characterization of **2**, DFT calculations using broken symmetry approach were performed with the B3LYP functional with D3 empirical dispersion, def2tzvp basis set, and PCM solvent model (THF). The spin density plot demonstrates that electronic structure of **2** involves a strong spin delocalization onto the bathocuproine ligands and thus supports the complex being a high spin iron(II) antiferromagnetically coupled to two ligand-based radicals in agreement with Anderson (Figure 4).

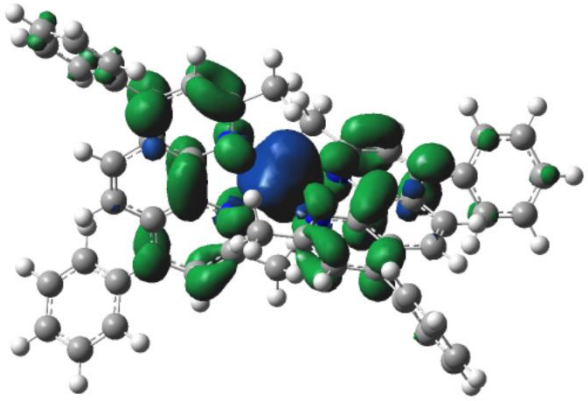

Figure 4: Spin density plot of **2** (positive spin density: blue, negative spin density: green).

*Use of **2** as an Alkyne Cycloaddition Catalyst*

Owing to its unsaturated nature, complex **2** appears to be a good candidate to undergo coordination of unsaturated C=C or C≡C bonds. Low-valent iron complexes (especially in the Fe^0 or Fe^I states) indeed display a good affinity for such unsaturated compounds, given the accessibility of the antibonding π* orbitals of the latter.[13] With this in mind, we anticipated that **2** would be a suitable platform for the activation of triple C≡C bonds, which led us to examine its catalytic efficacy in [2+2+2] alkyne cyclotrimerization. The use of 3rd-row transition metals as catalysts for such reactions is particularly appealing since this field is still strongly dominated by noble-metal-based catalysts,[14] and well-defined low-valent iron-based catalytic systems encompassing a large scope of alkyne cyclotrimerizations in mild conditions remain scarce, owing to the usual instability of such precursors.[15] An early report by Fürstner in 2008 showed that $CpFe^0(COD)•Li(MeOCH_2CH_2OMe)$ enables various cycloadditions, including alkyne [2+2+2] trimerization (toluene reflux, up to 24 h reaction time[15a]). Tilley also reported a rare dicoordinated heteroleptic Fe^I complex able to promote the cycloaddition of sterically non bulky

alkynes.[15b] More usually, ferrous precursors are used as precatalysts in alkyne cycloadditions, generation of the active species possibly proceeding by reduction using an external reductant such as a Grignard reagent[15d] or, as recently showed by Webster, by formation of transient iron hydrides.[15e] Recent reports by Jacobi von Wangelin also describe highly efficient cycloaddition systems relying on the use of $Fe^{II}(N(SiMe_3)_2)_2$ as a precursor, activated in the absence of external reductant[15c], or on the use of *in situ* generated reduced active species under photoredox conditions.[15f] Moreover, Roşca also recently described a method allowing the selective access to 1,3,5-substituted cycloadducts using a pyrimidinediimine-stabilized formal Fe^0 precursor.[15g]

Cycloaddition of phenylacetylene PhCCH (**3a**) was used as a benchmark reaction. In order to develop synthetic user-friendly conditions which could easily be carried out in the absence of a glovebox, **2** was generated by *in situ* reduction of **1** (by 2 equiv. Me_2C=CHMgBr in THF in the presence of a second equiv. of L), and **3a** was further added to the solution. In spite of the sterically crowded coordination sphere of the metal in **2**, the cyclotrimerization of **3a** proceeds with a 80% yield within 2 h at ambient temperature (Table 1, Entry 1), with a low 5 mol% catalytic charge. A near-quantitative yield is obtained using a higher catalytic load (10 mol%, Entry 2). Decreasing the charge of catalyst to lower quantities was detrimental to the reaction outcome (1 mol%, Entries 3-4). However, a near-quantitative yield is obtained with a 5 mol% catalyst charge after 2 h at 60 °C (Entry 7). It is of note that generation of **2** in the absence of a second equivalent of bathocuproine led to a much less efficient system since a 15 h reaction time and a 60 °C temperature were required to achieve a quantitative yield, and a slight loss of regioselectivity was observed (Entry 8). In all cases, the system displays a strong selectivity for the 1,2,4 isomer (1,2,4:1,3,5 = 98:2). Use of **1** as a catalyst in the absence of reductant did not

yield any cycloaddition product (Entry 9), confirming the necessity of a reduced iron catalyst. In line with this remark, when an isolated sample of **2** was used, a 98% cycloaddition yield was obtained (Entry 10). Moreover, when *in situ* generated Anderson's complex **2'** was used as a catalyst, significantly lower cycloaddition yields were obtained: 35% of **4a** were formed after 2 h at 60 °C (Entry 11), and 52% of **4a** were obtained after 2 h at room temperature (Entry 12). This poorer catalytic activity observed with the neocuproine-stabilized complex is in line with its lower thermic and kinetic stability when generated *in situ* (Figure 3). **2'** thus likely undergoes decomposition prior to achieving quantitative conversion of **3a**. On the other hand, in line with the better stability of **2'** when isolated as a pure solid prior to its utilization (*vide supra*, and Figure S10), a better catalytic activity is observed (95% yield, Entry 13). The use of $(phen)_2Fe^{II}Cl_2$ as an iron source reduced *in situ* with a Grignard also led to a modest 68% cycloaddition yield (Entry 14). The poorer results obtained using neocuproine and phenanthroline ligands instead of bathocuproine in *in situ* reducing conditions clearly demonstrate the importance of the substitution at the C4 and C7 positions in the stabilization of the *in situ* reduced iron species.

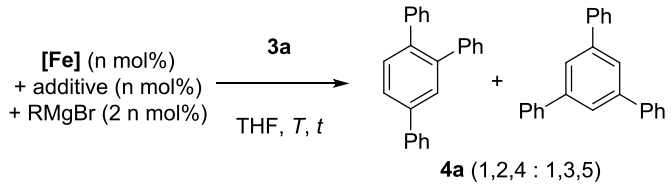

Entry	n (mol%)	**[Fe]** / additive	T (°C)	t (h)	Yield	1,2,4 : 1,3,5
1	5	**1** / L	r.t.	2	80	98 : 2
2	10	**1** / L	r.t.	3	98	> 99 : 1
3	1	**1** / L	r.t.	2	25	99 : 1
4	1	**1** / L	90	2	59	99 : 1
5	5	**1** / L	r.t.	3	85	98 : 2
6	5	**1** / L	50	2	88	98 : 2
7	5	**1** / L	60	2	98	99 : 1
8	5	**1** / no additive	60	15	99	91 : 9
9[a]	10	**1** / no additive	90	16	0	-
10[b]	5	**2** / no additive	60	2	98	99 : 1
11	5	**1'** / L'	60	2	35	99 : 1
12	5	**1'** / L'	r.t.	2	52	99 : 1
13[b]	5	**2'** / no additive	60	2	95	98 : 2
14	5	$(phen)Fe^{II}Cl_2$ / phen	60	2	68	99 : 1

Table 1 : optimization of the cyclotrimerization of PhCCH (**3a**) using **2** as an *in situ* generated catalyst; yields based on GC analysis (R = Me_2C=CH; L = bathocuproine; L' = neocuproine) ; [a] **1** was used as a catalyst in the absence of reductant; [b] a pure sample of **2** (Entry 10) or **2'** (Entry 13) was synthesized by reduction of **1** ($LFeCl_2$) or **1'** ($L'FeCl_2$) with KC_8 (2 equiv.) in THF, and used after removal of graphite and of the volatiles.

Given the facility to generate *in situ* complex **2** by reduction of **1** with a Grignard in the presence of one equivalent of bathocuproine and the encouraging cycloaddition results using phenylacetylene **3a** as a benchmark molecule, this system can provide a user-friendly procedure in synthetic chemistry. Indeed, no air-sensitive synthesis and purification of **2** is required prior to its use. The cycloaddition scope was then investigated (Scheme 3).

The same regioselectivity was observed regardless of the electronic nature of the aromatic substituents, since selective formation of the 1,2,4 cycloadduct isomer was observed starting from either electron-rich (*p*-Me, *p*-MeO, *p*-NH_2 – **3b**,**d**,**e**) or electron-poor (*p*-COOMe, *p*-Cl, *p*-F – **3f**,**g**,**h**) substituted substrates. It is of note that this method displays an appreciable functional group tolerance, since cycloadducts are quantitatively formed starting from phenylacetylenes substituted with trimethylsilyl groups (**3c**), ethers (**3d**), or C_{sp2}-F bonds (**3h**). Remarkably, several functionalities which are usually non-tolerant of reductive media are also tolerated, since moderate to good yields are obtained using primary amines (55%, **3e**), esters (66%, **3f**) or C_{sp2}-Cl bonds (59%, **3g**). Tolerance of acidic NH bonds in cycloadditions mediated by **2** is noteworthy since such substrates usually require deprotonative quench of the acidic NH protons prior to undergoing cycloaddition. Indeed, Webster reported that cycloaddition of *o*-$H_2NC_6H_4CCH$ promoted by a Fe^{II} / pinBH catalyst required the use of 2 equiv. pinBH to afford $N(Bpin)_2$ species prior to the cycloaddition.[15e] A good 81% yield was also obtained using the bulky naphthyl derivative **3i**, showing that this method can also encompass sterically crowded substrates. For those latter substrates (**3e**-**g**,**i**), a longer 24 h reaction time was applied.

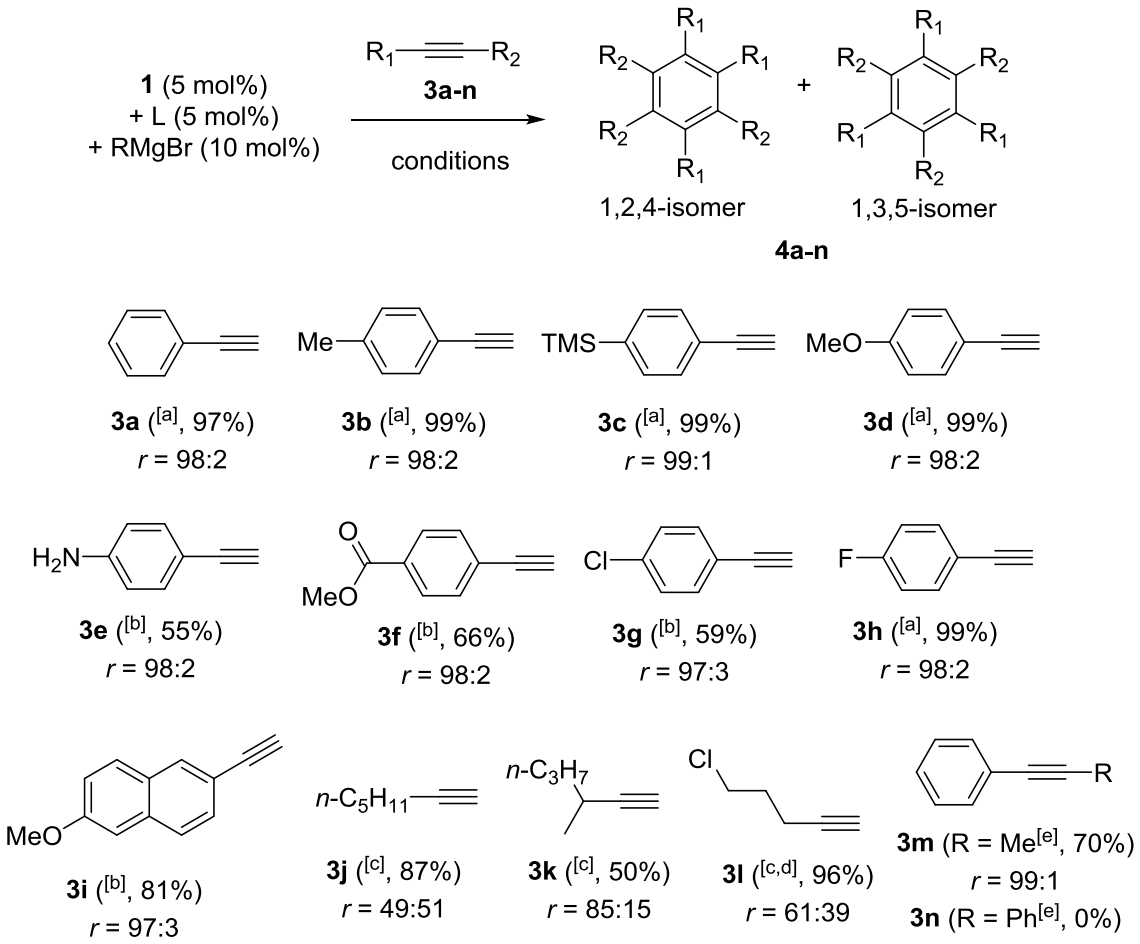

Scheme 3: Attempts of [2+2+2] cyclotrimerization on alkynes **3a**-**n** catalyzed by *in situ* formed **2**, generated by reduction of **1** in the presence of one equiv. L (L = bathocuproine) with 2 equiv. Me_2C=CHMgBr, in THF; isolated yields given between parentheses. [a] 60 °C, 2 h; [b] 60 °C, 24 h; [c]: 70 °C, 6 h; [d] **1** was reduced with 2 equiv. KC_8 in the presence of L, see SI; [e] conditions: 10 mol% **1**, 10 mol% L, 20 mol% RMgBr, 90 °C, 15 h; *r* = 1,2,4:1,3,5 ratio (evaluated by ^{1}H NMR after purification).

Terminal aliphatic alkynes such as 1-heptyne **3j** could also be efficiently converted. Slightly harder reaction conditions (6 h at 70 °C) were required to reach a 87% yield, and **4j** was obtained

as a 49:51 mixture of the 1,2,4 and 1,3,5 isomers. Conversion of aliphatic alkynes was found to be highly sensitive to steric hindrance, since the bulkier substrate **3k** only led to a 50% yield, with a pronounced preference for the 1,2,4 isomer (1,2,4:1,3,5 ratio = 85:15). It is also of note that 1-chloropent-4-yne (**3l**) was successfully transformed into the corresponding cycloadduct **4l** with an excellent 96% yield, showing that the presence of a reduced iron center in **2** is compatible with the presence of C_{sp3}-Cl bonds. In that case, **2** was generated *in situ* by reduction of **1** with 2 equiv. KC_8 and in the presence of a second equiv. of L (see SI), since a Cl/Br halogen metathesis on the C-Cl positions of **3l**/**4l** was partly observed when Me_2C=CHMgBr was used as a reductant. The tolerance of the methodology discussed herein for those functional groups thus promisingly opens the way for further post-functionalization transformations. Internal bulky alkynes often display a low reactivity in cyclotrimerization reactions and require high reaction temperatures.[15c] In line with this remark, 1-phenyl-1-propyne could afford the cycloadduct **4m** with a 70% yield in slightly harder conditions (Scheme 3). However, bulkier PhCCPh **3n** remained unchanged even at long reaction times at 90 °C.

Aiming at introducing more structural diversity using this methodology, we then investigated the feasibility of cross-cycloisomerization of 1,6-diynes with an external alkyne using **2** as an *in situ* generated catalyst (reduction of **1** by 2 equiv. Me_2C=CHMgBr in THF in the presence of a second equiv. of L). To our delight, the latter proved to be also an efficient catalyst for the cross-cycloaddition of 1,6-diynes such as **5** and **5'** with either aromatic, aliphatic, or internal alkynes (**3a**,**j**,**m**, Scheme 4).

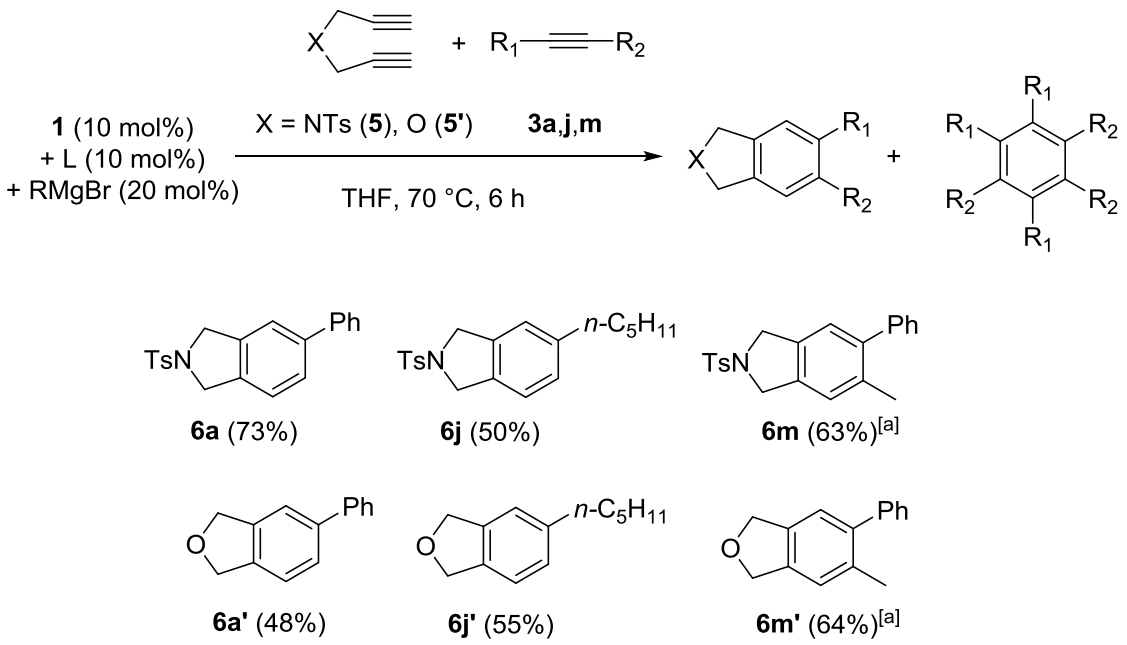

Scheme 4: [2+2+2] cross-cyclotrimerization between 1,6-diynes (**5** or **5'**) and alkynes (**3a**, **3j** and **3m**) catalyzed by *in situ* generated **2** (R = Me_2C=CH, L = bathocuproine) [a] : conditions: 15 h at 90 °C. Isolated yields given between parentheses.

It is noticeable that good yields could be obtained while using a strict 1:1 stoichiometry between the 1,6-diyne and the alkyne. An excess of the latter was indeed not required to achieve such yields, which is usually described in order to hamper the dimerization of the 1,6-diyne partner.[16] Interestingly, the yields obtained using internal alkyne PhCCMe (**3m**) as a cycloaddition partner with 1,6-diynes **5** and **5'** were higher than those obtained with 1-heptyne **3j** (63% (**6m**) *vs* 50% (**6j**) and 64% (**6m'**) *vs* 55% (**6j'**)). This increased reactivity in the cross-cyclotrimerization involving PhCCMe is mostly due to the slow competitive [2+2+2] cyclotrimerization rate of PhCCMe, which is less fast than that of 1-heptyne (Scheme 3, notes c and e).

The feasibility of [2+2+2] cocyclization of 1,6-diynes with alkynes mediated by **2** thus provides an access to various strategies for aromatic ring building using a cheap and non-toxic metal. Moreover, the system described herein relies on an easily accessible low-valent iron complex which requires a simple, commercially-available ligand, and generation of the active species proceeds without sacrificial consumption of alkyne starting material. Those examples are up to our knowledge amongst the rare examples of cross-cyclotrimerizations carried out using an iron-based catalyst, allowing moreover the use of this metal in attractive conditions (1:1 diyne:alkyne ratios, low catalytic charge, mild conditions).

Preliminary Mechanistic Insights for the Bathocuproine-Iron Cycloaddition

The last section of this report is devoted to the elucidation of several mechanistic insights of the cyclotrimerization catalytic process. The question of the nature of the active species in iron-mediated cycloaddition transformations is indeed pivotal in organometallic synthesis. Owing to the tendency of low iron oxidation states to form polynuclear reduced scaffolds,[17] several systems used in the past to carry out cycloaddition-based transformations proved to rely on the formation of reduced iron nanoparticles, formed from a well-defined precursor.[15c] It is also of note that few iron-based cycloaddition systems involve an active Fe^{II} species with no further reduction of the metal. Webster reported the example of alkyne cycloadditions mediated by an elusive Fe^{II} hydride formed by reaction of a Fe^{II}-salen precatalyst with pinacolborane. In the absence of formal structural characterization, implication of this Fe^{II}-H intermediate has been probed by deuteration experiments, and is sustained by DFT calculations.[15e,18]

From a mechanistic standpoint, a general consensus has been reached for alkyne [2+2+2] cycloaddition mediated by reduced transition metals, which involves a first oxidative coupling of two alkynes at the metal center.[19] Formation of this metallacycle is usually preceded by substitution of ancillary neutral ligands by the two incoming alkynes. Indeed, the active species which enters the catalytic cycle within the oxidative coupling step requires open coordination sites at the metal to accommodate the coordination of the two alkynes. The catalyst dormant state, reservoir of the active species, is on the other hand usually regenerated by reintroduction of the ancillary ligands in the metal coordination sphere. In the field of iron catalysis, an elegant representative example of ligand lability in [2+2+2] alkyne cycloaddition has recently been reported by Roşca.[15g] The authors describe the reactivity of a tridentate (N,N,N)Fe(N_2) species supported by a redox non-innocent pyrimidinediimine platform, which is used as a catalyst for alkyne [2+2+2] cycloadditions. In this system, a first alkyne enters the iron coordination sphere upon substitution with the ancillary N_2 ligand, whereas a decoordination of one arm of the (N,N,N) platform allows the coordination of the second alkyne, providing the formation of the expected ferracyclopentadiene.

On the basis of those considerations, we investigated the effect of the L:Fe ratio from the starting material in the cycloaddition conversions. According to the optimization work discussed in Table 1, the presence of a second equivalent of bathocuproine ligand enhances the catalytic activity of the iron in the cyclotrimerization process. When the transformation is carried out in the absence of bathocuproine (reduction of $FeCl_2$ by 2 equiv. Me_2C=CHMgBr), a slow conversion of phenylacetylene is still observed. The conversion rate quickly decreases and no evolution is observed after 6 h, with a small 35% conversion (Figure 5, (i)). This attests to the ability of transient reduced iron species to catalyze the [2+2+2] process, and those species likely evolve

towards the formation of unreactive reduced aggregates after several hours, due to the absence of stabilizing ligand. Use of **1** alone as a precatalyst leads to a more efficient and faster conversion (60% after 6 h, Figure 5, (ii)). Generation of **2** in the presence of the second equivalent of bathocuproine affords the best performance, since 100% conversion is observed after 1 h (Figure 5, (iii)).

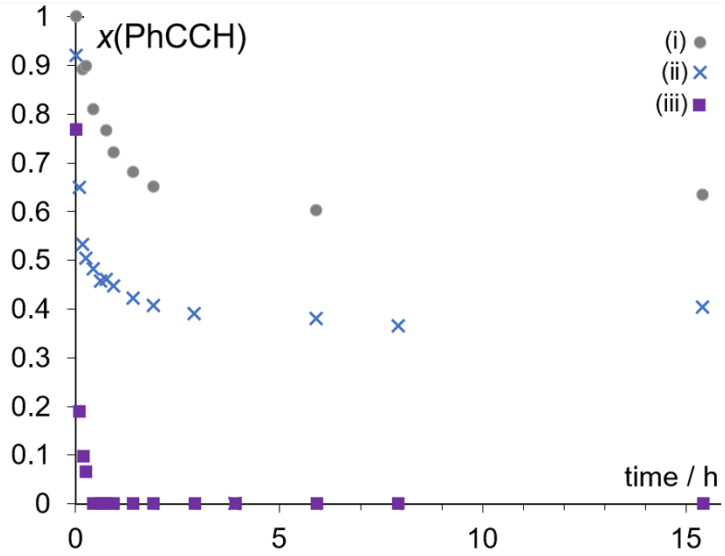

Figure 5: conversion of PhCCH (**3a**) at room temperature catalyzed by 0.1 equiv. of [Fe^{II}] precatalysts reduced by 2 equiv. Me_2C=CHMgBr in THF. [Fe^{II}] = $FeCl_2$ alone (i); **1** (ii); **1** + 1 equiv. L (iii).

It is remarkable that, in all cases showed in Figure 5, the conversion of **3a** occurs with no induction period, a catalytic activity being observed at short times. This is certainly indicative of a mechanism involving a well-defined reduced complex, with no implication of nanoparticles. Involvement of metal particles in a catalytic process usually indeed requires an induction period before the observation of any catalytic activity, characterized by a plateau-shaped curve at short times and an overall sigmoidal conversion profile.[20]

The faster conversion rate observed using the combination of **1** and one equiv. bathocuproine as a precatalytic system moreover suggests that either **2** is the active species able to initiate the cyclotrimerization process by the classic formation of a Fe^{II} ferracycle (Scheme 5a), or that **2** is a simple precatalyst, or a stabilized dormant state, of a more elusive mono-coordinated fragment LFe which would be the actual active species (Scheme 5b). In a second time, we thus aimed at rationalizing the L:Fe ratio (L:Fe = 2, 1 or 0) present in the species formed by reaction of **2** with PhCCH.

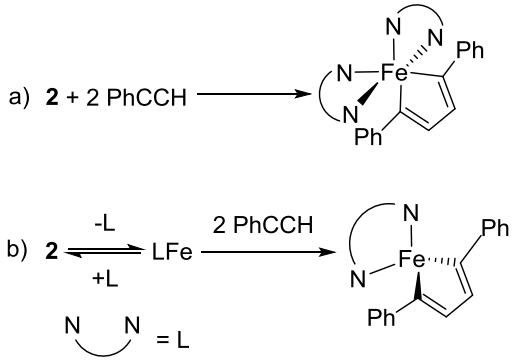

Scheme 5 : two possible initiation paths for the cyclotrimerization of PhCCH (**3a**) mediated by **2**, involving a) **2** as an active species or b) **2** as a precatalyst.

Using **2** as a pre-formed precatalyst, we wanted to identify which iron species were present during the trimerization by taking freeze-trapped Mössbauer samples at various timepoints during the catalytic reaction. The reaction of 10 equiv. of PhCCH to *in situ*-generated **2** at room temperature resulted in the loss of complex **2** and formation of two new iron species over time with parameters resembling Fe^0 (Figure S7). Note that no iron species were observed by 10 K EPR spectroscopy. While those two species are unable to be unambiguously assigned with the

current data and lack of a crystal structure despite extensive efforts, this observation indicates the ability of **2** to enter the catalytic cycle, potentially via substitution of a bathocuproine ligand by either an alkenyl ligand derived from the Grignard reagent or by PhCCH coordination to Fe^0.

To investigate this possibility, the catalytic reaction with PhCCH was performed at -30 ˚C, both with and without the presence of extra bathocuproine ligand to observe the effect of the amount of ligand present on the iron intermediates that are formed. Complex **2** was generated *in situ* from **1** in the presence of one additional equivalent of L at room temperature, after which the solution was cooled to -30 ˚C and 10 equiv. of PhCCH were added (Figure 6A). After 1 min of reaction, the consumption of **2** is observed with the concomitant formation of a new iron species (**7**) characterized by Mössbauer parameters of δ = 0.69 mm/s and $|\Delta E_Q|$ = 2.00 mm/s (77% of total iron, orange species). Alternatively, the reaction with only one equivalent of bathocuproine per mole of Fe was evaluated by adding 10 equiv. of PhCCH to a solution of **1** in THF at room temperature, followed by the cooling to -30 ˚C and the subsequent addition of 2 equiv. of alkenyl Grignard reagent (Figure 6B). In the absence of the second equivalent of bathocuproine, it was important to avoid ligand disproportionation affording 50% of iron nanoparticles and 50% of **2** after reduction of **1** by RMgBr (Fig. S4). Therefore, reduction of **1** was performed in that case in the presence of PhCCH (no traces of PhCC-CCPh were detected under those conditions and $Me_2C{=}CHCH{=}CMe_2$ was detected as **1** reduction byproduct, confirming the proficiency of the reduction of **1** by $Me_2C{=}CHMgBr$ in the presence of PhCCH). The freeze-trapped Mössbauer spectrum recorded 30 s after the Grignard addition also indicated in those conditions the analogous formation of **7** (91% of total iron, orange species, Figure 6B).

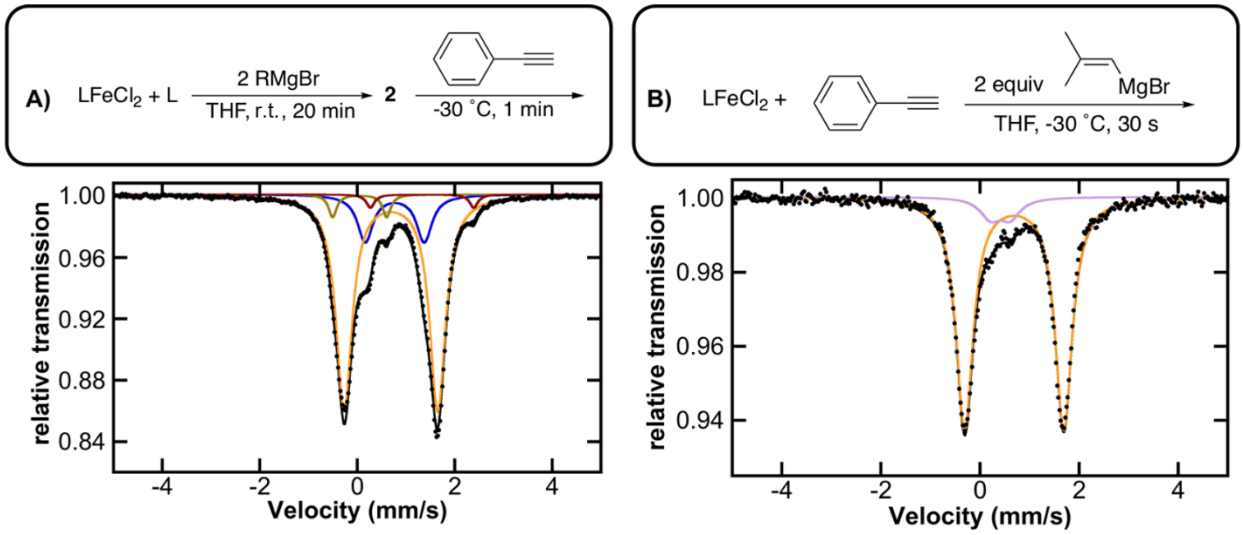

Figure 6: 80 K ^{57}Fe Mössbauer spectra of frozen solutions during trimerization of PhCCH at -30 ˚C mediated by **1** as a precatalyst A) with extra bathocuproine ligand and B) without extra bathocuproine ligand; raw data (black dots), total fit (black trace), individual fit components are shown; RMgBr = Me_2C=CHMgBr).

Since the same species **7** is formed after reduction of **1** in a high yield in the presence (77%) or the absence (91%) of a second equivalent of L, this strongly suggests that **7** does not feature a 2:1 L:Fe ratio, suggesting the formation of a 1:1 L:Fe complex. Importantly, this also shows that the same species **7** is formed by reduction of **1** in the presence of PhCCH, or by reaction of pre-formed **2** with PhCCH. While **7** may represent a bathocuproine-iron(0)-alkyne complex, no crystal structure could be obtained in order to unambiguously define this species. Regardless, this supports the formation of an iron intermediate in the presence of alkyne substrate with at most one ligand of bathocuproine bound, suggesting the potential formation of similar species at catalytic temperatures. Therefore, it is likely that, when **2** is formed prior to addition of the alkyne (reduction of **1** in the presence of a second equivalent of L, Figure 6A), addition of an excess of the alkyne induces a substitution of one bathocuproine ligand by two alkynes, such

ligand substitution being usually observed when a well-defined reduced metal complex is *per se* used as a starting material.[19] This would thus lead after oxidative coupling to the formation of an on-cycle metallacycle with a L:Fe = 1 ratio (Scheme 5b), similarly to what was described by Roşca for (N,N,N)Fe(N_2) species. In Roşca's system, the latter complex undergoes a loss of the ancillary N_2 ligand and partial decoordination of one arm of the (N,N,N) ligand prior to reacting with two equivalents of alkyne, also leading to a tetracoordinated (N,N)-ligated metallacycle after oxidative coupling.[15g] On the other hand, when **1** is reduced in the absence of a second equivalent of bathocuproine and in the presence of PhCCH (Figure 6B), a transient mono-coordinated reactive fragment LFe is likely formed, and readily accommodates the coordination of two alkynes to directly afford the corresponding metallacycle, keeping the L:Fe = 1 ratio, and bypassing the formation of **2**. In both cases, regardless of the presence or the absence of the second equivalent of bathocuproine, the same sole species **7** is detected by Mössbauer spectroscopy (Figure 6A-B). Therefore, **2** appears as a good precursor for generating low-coordinated reactive fragments in cycloaddition conditions, by loss of one bathocuproine ligand in the presence of an alkyne. It can be anticipated that, at the end of the cycloaddition process – that is, for small alkyne:Fe ratios, **2** may be a stable iron dormant state which precludes iron evolution towards unreactive aggregates, as highlighted by the conversion profiles discussed in Figure 5: alkyne conversion is indeed complete when a L:Fe = 2 ratio is used in the starting material (Figure 5-iii).

The possible lability of a bathocuproine ligand of complex **2** in the presence of an alkyne has moreover been strengthened by DFT calculations. Overall formation of a high-spin Fe^{II} metallacycle ^{5}**A** by oxidative coupling of two equivalents of PhCCH with release of one equivalent of bathocuproine from **2** proved to be thermally feasible, since an exergonicity of ca.

30 kcal.mol^{-1} was calculated for this transformation (Scheme 6a). In the absence of formal structural characterization of the metallacycle intermediate in this cycloaddition system, those calculations at least suggest that implication of under-coordinated structures involving iron cations stabilized by only one equivalent of bathocuproine can be thermally envisioned.

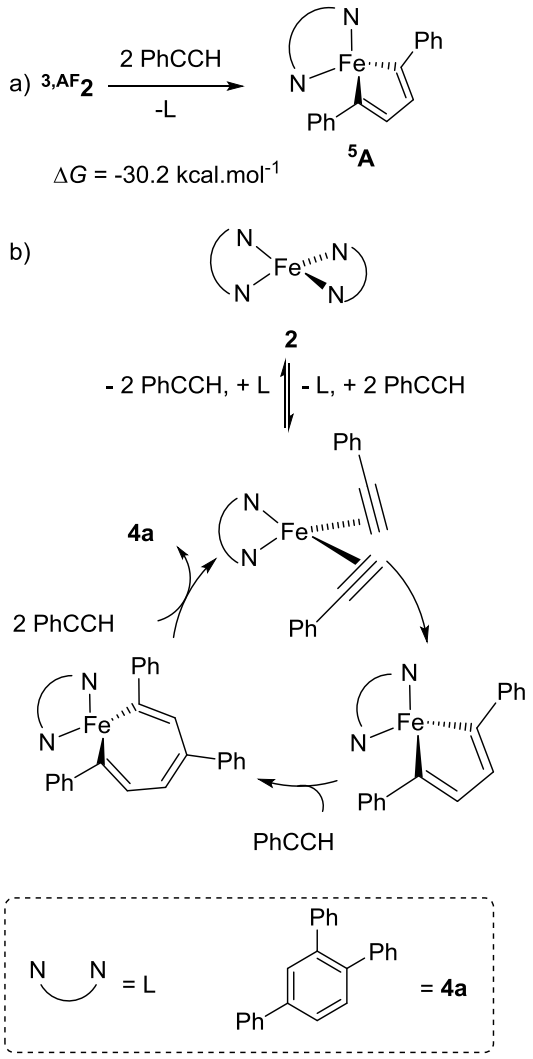

Scheme 6: a) oxidative coupling of two equivalents of PhCCH with ^{3,AF}**2** (featuring a high-spin Fe^{II} ion (S = 2) antiferromagnetically coupled (AF) to one unpaired electron onto each L ligand; L = bathocuproine); theory level: UB3LYP, PCM(THF), GD3 dispersion correction; spin

multiplicity superscripted; b) suggested catalytic cycle for cycloaddition of PhCCH (**3a**) into **4a** by *in situ* generated **2**, featuring the latter as a dormant state.

Decoordination of a bathocuproine ligand from complex **2** upon reaction with an excess of PhCCH has also been probed using cyclic voltammetry. **2** is characterized by two reduction peaks in DMF at E_p(R1) = -2.0 V *vs* $Fc^{0/+}$ and E_p(R2) = -2.4 V *vs* $Fc^{0/+}$, associated with oxidation peaks at E_p(O1) = -1.9 V *vs* $Fc^{0/+}$ and E_p(O2) = -2.2 V *vs* $Fc^{0/+}$ (Figure 7, plain lines (—) and see Figure S11 for the full cyclic voltammetry).

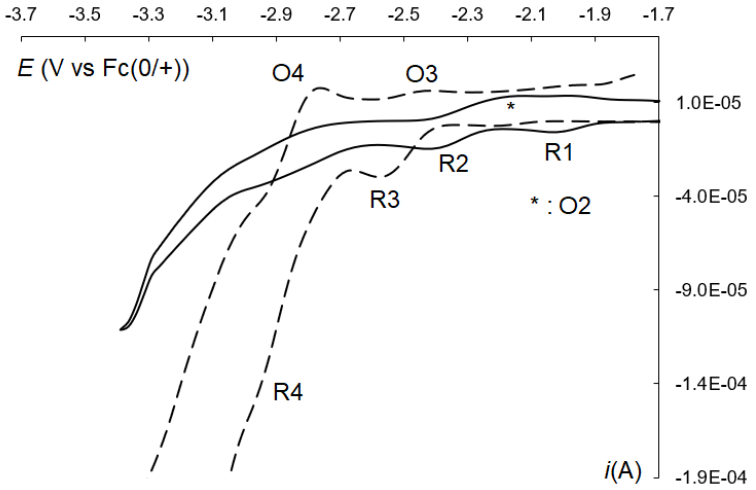

Figure 7: cyclic voltammetry, performed in DMF at a gold disk electrode (*d* = 2 mm) with nBu$_4$NBF$_4$ (0.2 M) as a supporting electrolyte, of a 2.5 mM solution of **2**, in the absence (—), or the presence of 20 equiv. of PhCCH (---); scan rate = 0.3 Vs^{-1}.

In the presence of an excess of PhCCH (20 equiv.) and after 5 minutes at room temperature, reduction peaks R1 and R2 disappear, attesting to the reaction of **2** with PhCCH (Figure 7, dashed lines (---)). Concomitantly, reduction peak R3 develops at E_p(R3) = -2.5 V *vs* $Fc^{0/+}$, associated with oxidation peak O3 at E_p(O3) = -2.4 V *vs* $Fc^{0/+}$, as well as reduction peak R4 at

E_p(R4) = -2.9 V *vs* $Fc^{0/+}$, associated with oxidation peak O4 at E_p(O4) = -2.8 V *vs* $Fc^{0/+}$ on the reverse scan. R4 is detected as a shoulder to the high reduction peak of the excess of PhCCH (E_p(R5) = -3.3 V *vs* $Fc^{0/+}$, see Figure S12 for the full voltammetry). Reversible systems R3/O3 and R4/O4 have been assigned to free bathocuproine, released in the reaction medium upon action of PhCCH on **2**, by comparison with the cyclic voltammetry of a pure sample of bathocuproine (see Figure S13). Overall, electrochemical analysis also points towards the decoordination of bathocuproine ligand from **2** upon reaction with PhCCH. In line with this, the use of an excess of ligand is detrimental to the outcome of the cycloaddition reaction, since only 75% cycloaddition yield is obtained when **1** is associated with 11 equiv. L at 60 °C during 2 h (to be compared with 98% when only 1 equiv. L is added, Table 1, Entry 7).

Moreover, another way **2** could enter the catalytic cycle is from the potential formation of an Fe^I species from the comproportionation of **1** and **2**. Freeze-trapped ^{57}Fe Mössbauer and EPR experiments upon reaction of equal amounts of **1** and **2** did not reveal the formation of any new iron species (including any Fe^I species) with only unreacted **1** and **2** observed, which was confirmed by room-temperature ^{1}H NMR analysis (Figures S8-9). This behavior is in contrast with several well reported nickel-mediated transformations, in which the catalytic cycle relies on key redox comproportionation steps.[9c]

The efficiency of the association of bathocuproine with a formal Fe^0 metal in alkyne cycloaddition likely originates in the π-acidic character of this ligand. Thanks to the transfer of some electronic density from the metal onto the π* system of the ligand, the alkyne can play the role of a σ-donating ligand, and easily enter the iron coordination sphere. The occurrence of the

cycloaddition process moreover demonstrates the availability of the electron density delocalized onto the bathocuproine scaffold, since the classic [2+2+2] mechanism involving formation of a ferracycle as a first step (Scheme 5) requires formal oxidation states lower than Fe^{II}. In the absence of structural characterization of intermediates obtained *in situ* during the cycloaddition process, preliminary experiments seem to suggest that, while **2** is able to promote the [2+2+2] alkyne cycloaddition, the loss of one bathocuproine ligand may be necessary to enter the catalytic cycle.[21] Those preliminary conclusions have been gathered on the tentative catalytic cycle showed in Scheme 6b.

CONCLUSION.

In conclusion, we demonstrated that phenanthroline-type ligands can be efficiently associated with formal iron(0) oxidation state to provide new thermally stable species. The interaction of this reduced metal with the ligand is dominated by a delocalization of the electronic charge onto the low-lying LUMOs of the non-innocent phen-type platform. For the first time, we show that such reduced Fe species with phen-type ligands can be stabilized by a steric protection of the C4 and C7 positions by hindered groups (such as Ph in the case of the bathocuproine ligand, L). The resulting L_2Fe complex (**2**) displays enhanced thermal and kinetic stabilities in solution, especially when generated *in situ* by reduction of the suitable precursor in standard synthetic conditions (e.g. use of a Grignard reagent), and can act as an efficient dormant state, reservoir of the *in situ* generated active species, in low-valent iron-mediated catalytic processes.

From a practical standpoint, the ferrous precursor of **2** (**1**) proved to be bench-stable and did not undergo any degradation when stored under ambient atmosphere for several weeks. Since *in situ*

reduction of **1** quantitatively affords thermally stable complex **2** in the presence of one additional equivalent of bathocuproine, **1** appears as an easily handled precursor for potential catalytic applications relying on low iron oxidation states. Those results also show that *in situ* generated **2** can be used in atom-economical and efficient C-C bond formation processes to access functionalized aromatic rings, and that a variety of partners can be encompassed depending on the chosen strategy. [2+2+2] trimerization or cocyclization of alkynes are indeed easily promoted using **2** as a precatalyst.

AUTHOR INFORMATION

Corresponding Author

*E-mail: guillaume.lefevre@chimieparistech.psl.eu; michael.neidig@rochester.edu.

Notes

The authors declare no competing financial interests.

ASSOCIATED CONTENT

Supporting information (PDF): general procedures, ^{1}H, ^{13}C, ^{19}F NMR and Mössbauer spectra, theoretical methods, cartesian coordinates of the computed structures, SQUID magnetometry plots, electrochemical methods, crystallographic data. CCDC 2149974−2149975 contain the supplementary crystallographic data for this paper. The corresponding files are available free of charge.

REFERENCES.

[1] a) Small, B. L.; Brookhart, M. Iron-Based Catalysts with Exceptionally High Activities and Selectivities for Oligomerization of Ethylene to Linear α-Olefins. *J. Am. Chem. Soc.* **1998**, *120*, 7143–7144. doi.org/10.1021/ja981317q; b) J. P. Britovsek, G.; C. Gibson, V.; J. McTavish, S.; A. Solan, G.; J. P. White, A.; J. Williams, D.; J. P. Britovsek, G.; S. Kimberley, B.; J. Maddox, P. Novel Olefin Polymerization Catalysts Based on Iron and Cobalt. *Chem. Commun.* **1998**, *7*, 849–850. doi.org/10.1039/A801933I.

[2] a) de Bruin, B.; Bill, E.; Bothe, E.; Weyhermüller, T.; Wieghardt, K. Molecular and Electronic Structures of Bis(Pyridine-2,6-Diimine)Metal Complexes [ML2](PF6)n (n = 0, 1, 2, 3; M = Mn, Fe, Co, Ni, Cu, Zn). *Inorg. Chem.* **2000**, *39*, 2936–2947. doi.org/10.1021/ic000113j; b) Budzelaar, P. H. M.; de Bruin, B.; Gal, A. W.; Wieghardt, K.; van Lenthe, J. H. Metal-to-Ligand Electron Transfer in Diiminopyridine Complexes of Mn−Zn. A Theoretical Study. *Inorg. Chem.* **2001**, *40*, 4649–4655. doi.org/10.1021/ic001457c; c) Scott, J.; Gambarotta, S.; Korobkov, I.; Knijnenburg, Q.; de Bruin, B.; Budzelaar, P. H. M. Formation of a Paramagnetic Al Complex and Extrusion of Fe during the Reaction of (Diiminepyridine)Fe with AlR3 (R = Me, Et). *J. Am. Chem. Soc.* **2005**, *127*, 17204–17206. doi.org/10.1021/ja056135s; d) Scott, J.; Gambarotta, S.; Korobkov, I.; Budzelaar, P. H. M. Reduction of (Diiminopyridine)Iron: Evidence for a Noncationic Polymerization Pathway? *Organometallics* **2005**, *24*, 6298–6300. doi.org/10.1021/om0507833; e) Enright, D.; Gambarotta, S.; Yap, G. P. A.; Budzelaar, P. H. M. The Ability of the α,A′-Diiminopyridine Ligand System to Accept Negative Charge: Isolation of Paramagnetic and Diamagnetic Trianions. *Angew. Chem. Int. Ed.* **2002**, *41*, 3873–3876. doi.org/10.1002/1521-3773(20021018)41:20<3873::AIDANIE3873>3.0.CO;2-8.

[3] Bart, S. C.; Lobkovsky, E.; Chirik, P. J. Preparation and Molecular and Electronic Structures of Iron(0) Dinitrogen and Silane Complexes and Their Application to Catalytic Hydrogenation and Hydrosilation. *J. Am. Chem. Soc.* **2004**, *126*, 13794–13807. doi.org/10.1021/ja046753t.

[4] Sylvester, K. T.; Chirik, P. J. Iron-Catalyzed, Hydrogen-Mediated Reductive Cyclization of 1,6-Enynes and Diynes: Evidence for Bis(Imino)Pyridine Ligand Participation. *J. Am. Chem. Soc.* **2009**, *131*, 8772–8774. doi.org/10.1021/ja902478p.

[5] Lee, H.; Campbell, M. G.; Hernández Sánchez, R.; Börgel, J.; Raynaud, J.; S. E.; Ritter, T. Mechanistic Insight into High-Spin Iron(I)-Catalyzed Butadiene Dimerization. *Organometallics* **2016**, *25*, 27, 2923-2929. doi.org/10.1021/acs.organomet.6b00474.

[6] a) Braconi, E.; Götzinger, A. C.; Cramer, N. Enantioselective Iron-Catalyzed Cross-[4+4]-Cycloaddition of 1,3-Dienes Provides Chiral Cyclooctadienes. *J. Am. Chem. Soc.* **2020**, *142*, 19819–19824.doi.org/10.1021/jacs.0c09486; b) Vraconi, E.; Cramer, N. Crossed Regio- and Enantioselective Iron-Catalyzed [4+2]-Cycloadditions of Unactivated Dienes. *Angew. Chem. Int. Ed.* **2022**, *61*, e202112148.doi.org/https://doi.org/10.1002/anie.202112148.

[7] Maier, T. M.; Gawron, M.; Coburger, P.; Bodensteiner, M.; Wolf, R.; van Leest, N. P.; de Bruin, B.; Demeshko, S.; Meyer, F. Low-Valence Anionic α-Diimine Iron Complexes: Synthesis, Characterization, and Catalytic Hydroboration Studies. *Inorg. Chem.* **2020**, *59*, 16035–16052. doi.org/10.1021/acs.inorgchem.0c02606

[8] Bart, S. C.; Chlopek, K.; Bill, E.; Bouwkamp, M. W.; Lobkovsky, E.; Neese, F.; Wieghardt, K.; Chirik, P. J. Electronic Structure of Bis(imino)pyridine Iron Dichloride, Monochloride, and Neutral Ligand Complexes: A Combined Structural, Spectroscopic, and Computational Study. *J. Am. Chem. Soc.* **2006**, *128*, 42, 13901-13912. doi.org/10.1021/ja064557b.

[9] a) Lyaskovskyy, V.; de Bruin, B. Redox Non-Innocent Ligands: Versatile New Tools to ControlCatalytic Reactions. *ACS Catal*. **2012**, *2*, 270-279. https://doi.org/10.1021/cs200660v; b) de Bruin, B.; Gualco, P.; Paul, N. D. Redox Non-Innocent Ligands: Reactivity and Catalysis. In *Ligand Design in Metal Chemistry: Reactivity and Catalysis*; 2016; pp 176-204; c) Diccianni, J.; Lin, Q.; Diao, T. Mechanisms of Nickel-Catalyzed Coupling Reactions and Applications in Alkene Functionalization. *Acc. Chem. Res.* **2020**, *54*, 4, 906-919. doi.org/10.1021/acs.accounts.0c00032; d) Hu, M.-Y.; He, Q.; Fan, S.-J.; Wang, Z.-C.; Liu, L.-Y.; Mu, Y.-J.; Peng, Q.; Zhu, S.-F. Ligands with 1,10-phenanthroline scaffold for highly regioselective iron-catalyzed alkene hydrosilylation. *Nature Comm.* **2018**, *9*, 221, https://doi.org/10.1038/s41467-017-02472-6; e) Guo, N.; Hu, M.-Y.; Feng, Y.; Zhu, S.-F. Highly efficient and practical hydrogenation of olefins catalyzed by in situ generated iron complex catalysts. *Org. Chem. Front.* **2015**, *2*, 692-696. DOI: 10.1039/c5qo00064e.

[10] For examples of such radical-based reactivities in rare-earth phen complexes, see a) Nocton, G.; Lukens, W. L.; Booth, C. H.; Rozenel, S. S.; Melding, S. A.; Maron, L.; Andersen, R. A. Reversible Sigma C–C Bond Formation Between Phenanthroline Ligands Activated by $(C_5Me_5)_2Yb$. *J. Am. Chem. Soc*. **2014**, *136*, 8626-8641. doi.org/10.1021/ja502271q; b) Nocton, G.; Ricard, L. Reversible C–C coupling in phenanthroline complexes of divalent samarium and thulium. *Chem. Commun*., **2015**, *51*, 3578-3581. doi.org/10.1039/C5CC00289C.

[11] Jesse, K. A.; Filatov, A. S.; Xie, J.; Anderson, J. S. Neocuproine as a Redox-Active Ligand Platform on Iron and Cobalt. *Inorg. Chem*. **2019**, *58*, 9057-9066. doi.org/10.1021/acs.inorgchem.9b00531.

[12] a) Daifuku, S. L.; Kneebone, J. L.; Snyder, B. E. R.; Neidig, M. L. Iron(II) Active Species in Iron-Bisphosphine Catalyzed Kumada and Suzuki-Miyaura Cross-Couplings of Phenyl Nucleophiles and Secondary Alkyl Halides. *J. Am. Chem. Soc*. **2015**, *137*, 11432–11444. doi.org/10.1021/jacs.5b06648; b) Kneebone, J. L.; Fleischauer, V. E.; Daifuku, S. L.; Shaps, A. A.; Bailey, J. M.; Iannuzzi, T. E.; Neidig,

M. L. Electronic Structure and Bonding in Iron(II) and Iron(I) Complexes Bearing Bisphosphine Ligands of Relevance to Iron-Catalyzed C–C Cross-Coupling. *Inorg. Chem.* **2016**, *55*, 272–282. doi.org/10.1021/acs.inorgchem.5b02263; c) Kneebone, J. L.; Brennessel, W. W.; Neidig, M. L. Intermediates and Reactivity in Iron-Catalyzed Cross-Couplings of Alkynyl Grignards with Alkyl Halides. *J. Am. Chem. Soc.* **2017**, *139*, 20, 6988–7003. doi.org/10.1021/jacs.7b02363.

[13] a) Cheng, J.; Chen, Q.; Leng, X.; Ye, S.; Deng, L. Three-Coordinate Iron(0) Complexes with N-Heterocyclic Carbene and Vinyltrimethylsilane Ligation: Synthesis, Characterization, and Ligand Substitution Reactions. *Inorg. Chem*. **2019**, *58*, 19, 13129–13141. doi.org/10.1021/acs.inorgchem.9b02009; b) Wang, L.; Cheng, J.; Ma, Y.; Chen, Q.; Leng, X.; Deng, L. Three-coordinate Bis(N-heterocyclic carbene)iron(0) complexes with alkene and alkyne ligation: Synthesis and characterization. *Polyhedron* **2021**, *197*, 115054-115062. doi.org/10.1016/j.poly.2021.115054.

[14] Selected reviews: a) Vollhardt, K. P. C. Cobalt-mediated [2 + 2 + 2]-cycloadditions: a maturing synthetic strategy. *Angew. Chem. Int. Ed.* **1984**, *23*, 539-556; b) Varela, J. A.; Saá, C. Construction of pyridine rings by metal-mediated [2 + 2 + 2] cycloaddition. *Chem. Rev.* **2003**, *103*, 3787-3802; c) Chopade, P. R.; Louie, J. [2+2+2] Cycloaddition reactions catalyzed by transition metal complexes. *Adv. Synth. Catal.* **2006**, *348*, 2307-2327; d) Gandon, V.; Aubert, C.; Malacria, M. Recent progress in cobalt-mediated [2 + 2 + 2] cycloaddition reactions. *Chem. Commun*., **2006**, 2209-2217; e) Marinetti, A.; Jullien, H.; Voituriez, A. Enantioselective, transition metal catalyzed cycloisomerizations. *Chem. Soc. Rev.* **2012**, *41*, 4884-4908. doi.org/10.1039/C2CS35020C; f) Matton, P.; Huvelle, S.; Haddad, M.; Phansavath, P.; Ratovelomanana-Vidal, V. Recent Progress in Metal-Catalyzed [2+2+2] Cycloaddition Reactions. *Synthesis* **2022**, *54*, 4-32. DOI:10.1055/s-0040-1719831.

[15] a) Fürstner, A.; Majima, K.; Martin, R.; Krause, H.; Kattnig, E.; Goddard, R.; Lehmann, C. W. A Cheap Metal for a "Noble" Task: Preparative and Mechanistic Aspects of Cycloisomerization and Cycloaddition Reactions Catalyzed by Low-Valent Iron Complexes. *J. Am. Chem. Soc*. **2008**, *130*, 6, 1992–2004. doi.org/10.1021/ja0777180; b) Lipschutz, M. I.; Chantarojsiri, T.; Dong, Y.; Don Tilley, T. Synthesis, Characterization and Alkyne Trimerization Catalysis of a Heteroleptic Two-Coordinate Fe^{I} Complex. *J. Am. Chem. Soc.* **2015**, *137*, 19, 6366–6372. doi.org/10.1021/jacs.5b02504; c) Brenna, D.; Villa, M.; Gieshoff, T. N.; Fischer, F.; Hapke, M.; Jacobi von Wangelin, A. Iron-Catalyzed Cyclotrimerization of Terminal Alkynes by Dual Catalyst Activation in the Absence of Reductant. *Angew. Chem. Int. Ed*. **2017**, *56*, 8451–8454. doi.org/10.1002/anie.201705087; d) Gawali, S. S.; Gunanathan, C. Iron-catalyzed regioselective cyclotrimerization of alkynes to benzenes, *J. Organomet. Chem*. **2019**, *881*, 139-149; e) Provis-Evans, C. B.; Lau, S.; Krewald, V.; Webster, R. L. Regioselective Alkyne Cyclotrimerization with an In Situ-Generated [Fe(II)H(salen)]·Bpin Catalyst. *ACS Catal*. **2020**, *10*, 17, 10157–10168. doi.org/10.1021/acscatal.0c03068; f) Neuemeier, M.; Chakraborty, U.; Schaarschmidt, D.; de la Pena O'Shea, V.; Perez-Ruiz, R.; Jacobi von Wangelin, A Combined Photoredox and Iron Catalysis for the Cyclotrimerization of Alkynes. *Angew. Chem. Int. Ed*. **2020**, *59*, 13473−13478; g) Doll, J. S.; Eichelmann, R.; Hertwig, L. E.; Bender, T.; Kohler, V. J.; Bill, E.; Wadepohl, H.; Roşca, D.-A. Iron-Catalyzed Trimerization of Terminal Alkynes Enabled by Pyrimidinediimine Ligands: A Regioselective Method for the Synthesis of 1,3,5-Substituted Arenes. *ACS Catal.*, **2021**, *11*, 9, 5593-5600. doi.org/10.1021/acscatal.1c00978.

[16] Ye, F.; Haddad, M.; Michelet, V.; Ratovelomanana-Vidal, V. Access toward Fluorenone Derivatives through Solvent-Free Ruthenium Trichloride Mediated [2 + 2 + 2] Cycloadditions. *Org. Lett*. **2016**, *18*, 5612−5615. doi.org/10.1021/acs.orglett.6b02840.

[17] Muñoz III, S. B.; Daifuku, S. L.; Brennessel, W. W.; Neidig, M. L. Isolation, Characterization, and Reactivity of $Fe_8Me_{12}^-$: Kochi's S = 1/2 Species in Iron-Catalyzed Cross-Couplings with MeMgBr and Ferric Salts. *J. Am. Chem. Soc*. **2016**, *138*, 7492–7495. doi.org/10.1021/jacs.6b03760.

[18] For another example of well-defined Fe^{II} platform allowing [2+2+2] alkyne cycloaddition, see Frazier, B. A.; Williams, V. A.; Wolczanski, P. T.; Bart, S. C.; Meyer, K.; Cundari, T. R.; Lobkovsky, E. B. C−C Bond Formation and Related Reactions at the CNC Backbone in (smif)FeX (smif = 1,3-Di-(2-pyridyl)-2-azaallyl): Dimerizations, 3 + 2 Cyclization, and Nucleophilic Attack; Transfer Hydrogenations and Alkyne Trimerization (X = $N(TMS)_2$, dpma = (Di-(2-pyridyl-methyl)-amide)). *Inorg. Chem*. **2013**, *52*, 3295-3312. doi.org/10.1021/ic302783y.

[19] Roglans, A.; Pla-Quintana, A.; Solà, M. Mechanistic Studies of Transition-Metal-Catalyzed [2 + 2 + 2] Cycloaddition Reactions. *Chem. Rev*. **2021**, *121*, 3, 1894–1979. doi.org/10.1021/acs.chemrev.0c00062.

[20] Widegren, J. A.; Finke, R. G. A review of the problem of distinguishing true homogeneous catalysis from soluble or other metal-particle heterogeneous catalysis under reducing conditions. *Journal of Molecular Catalysis A: Chemical* **2003**, *198*, 317-341. doi.org/10.1016/S1381-1169(02)00728-8.

[21] Addition of an excess of the bulky alkyne PhCCPh on *in situ* generated **2** leads to the formation of a new minor paramagnetic species detected in ^{1}H NMR (Figure S6). Given that no conversion of PhCCPh is observed in cycloaddition conditions (Scheme 3), this might suggest that coordination of the alkyne at the iron is also possible for bulky substrates, but that the oxidative coupling is in that case hampered for steric reasons.

Author Contributions

The manuscript was written through contributions of all authors. All authors have given approval to the final version of the manuscript.

Funding Sources

G.L. thanks the ERC (Project DoReMI StG, 852640) for its financial support. M.L.N acknowledges the National Institutes of Health (R01GM111480) for its financial support. Dr F. Lagroix (Institut de Physique du Globe de Paris) is thanked for technical assistance and fruitful discussions. The authors thank the CNRS and the MESRI for financial support. The NMR shared facilities of Chimie ParisTech are thanked for technical support. The authors also wish to acknowledge the MS3U platform of Sorbonne Université for the HRMS analyses. Dr. I. Ciofini and Prof. C. Adamo (Chimie ParisTech) are thanked for access to computational facilities.

For table of contents only